

High potential for CH₄ emission mitigation from oil infrastructure in one of EU's major production regions

Foteini Stavropoulou^{1,*}, Katarina Vinković^{2,*}, Bert Kers², Marcel de Vries², Steven van Heuven², Piotr Korbeń³, Martina Schmidt³, Julia Wietzel³, Pawel Jagoda⁴, Jaroslav M. Necki⁴, Jakub Bartyzel⁴, Hossein Maazallahi¹, Malika Menoud¹, Carina van der Veen¹, Sylvia Walter¹, Béla Tuzson⁵, Jonas Ravelid⁵, Randolph Paulo Morales⁵, Lukas Emmenegger⁵, Dominik Brunner⁵, Michael Steiner⁵, Arjan Hensen⁶, Ilona Velzeboer⁶, Pim van den Bulk⁶, Hugo Denier van der Gon⁶, Antonio Delre⁷, Maklawe Essonanawe Edjabou⁷, Charlotte Scheutz⁷, Marius Corbu^{8,9}, Sebastian Iancu⁹, Denisa Moaca⁹, Alin Scarlat^{8,9}, Alexandru Tudor^{8,9}, Ioana Vizireanu⁹, Andreea Calcan⁹, Magdalena Ardelean⁹, Sorin Ghemulet⁹, Alexandru Pana⁹, Aurel Constantinescu⁹, Lucian Cusa⁹, Alexandru Nica⁹, Calin Baciu¹⁰, Cristian Pop¹⁰, Andrei Radovici¹⁰, Alexandru Mereuta¹⁰, Horatiu Stefanie¹⁰, Bas Hermans¹¹, Stefan Schwietzke¹², Daniel Zavala-Araiza^{1, 12}, Huilin Chen^{2, 13**}, Thomas Röckmann^{1,**}

¹Institute for Marine and Atmospheric Research Utrecht (IMAU), Utrecht University, the Netherlands

²Centre for Isotope Research (CIO), Energy and Sustainability Research Institute Groningen, University of Groningen, The Netherlands

³Institute of Environmental Physics, University of Heidelberg, Heidelberg, Germany

⁴Faculty of Physics and Applied Computer Science, AGH University of Science and Technology in Cracow, Cracow, Poland

⁵Laboratory for Air Pollution/Environmental Technology, Empa – Swiss Federal Laboratories for Materials Science and Technology, Überlandstrasse 129, CH-8600 Dübendorf

⁶Department of Environmental Modelling, Sensing & Analysis, TNO, the Netherlands

⁷Department of Environmental Engineering, Technical University of Denmark, Denmark

⁸ Faculty of Physics, University of Bucharest, P.O. Box MG-11, Magurele, 077125, Bucharest, Romania

⁹ National Institute for Aerospace Research “Elie Carafoli” – INCAS Bucharest, Romania

¹⁰Faculty of Environmental Science and Engineering, Babes-Bolyai University, Cluj-Napoca, Romania

¹¹ Intero - The Sniffers, Poeierstraat 14, 2490 Balen, Belgium

¹²Environmental Defense Fund, Berlin, Germany and Amsterdam, The Netherlands

¹³Joint International Research Laboratory of Atmospheric and Earth System Sciences, School of Atmospheric Sciences, Nanjing University, Nanjing, China

* These authors contributed equally to the manuscript

** corresponding authors

Abstract

Ambitious methane (CH₄) emissions mitigation represents one of the most effective opportunities to slow the rate of global warming over the next decades. The oil and gas (O&G) sector is a significant source of methane emissions, with technically feasible and cost-effective emission mitigation options. Romania, a key O&G producer within the EU, with the second highest reported annual CH₄ emissions from the energy sector in year 2020 (Greenhouse Gas Inventory Data - Comparison by Category, 2022), can play an important role towards the EU's

48 emission reduction targets. In this study, we quantify CH₄ emissions from onshore oil
49 production sites in Romania at source and facility level using a combination of ground and
50 drone-based measurement techniques. Measured emissions were characterised by heavily
51 skewed distributions, with 10% of the sites accounting for more than 70% of total emissions.
52 Integrating the results from all site-level quantifications with different approaches, we derive
53 a central estimate of 5.4 kg h⁻¹ site⁻¹ of CH₄ (3.6 – 8.4, 95% confidence interval) for oil
54 production sites. This estimate represents the third highest when compared to measurement-
55 based estimates of similar facilities from other production regions. Based on our results, we
56 estimate a total of 120 ktons CH₄ yr⁻¹ (range: 79 - 180 ktons yr⁻¹) from oil production sites in
57 our studied areas in Romania. This is approximately 2.5 times higher than the reported
58 emissions from the entire Romanian oil production sector for 2020. Based on the source level
59 characterization, up to three quarters of the detected emissions from oil production sites are
60 related to operational venting. Our results suggest that O&G production infrastructure in
61 Romania holds a massive mitigation potential, specifically by implementing measures to
62 capture the gas and minimize operational venting and leaks.
63 **Keywords:** Methane emissions; Oil and gas sector; Emissions distributions; Ground-based
64 measurements; Romania; Mitigation;

65 1. Introduction

66 CH₄, a potent greenhouse gas, is more effective at trapping radiation than CO₂, but has a
67 shorter lifetime. CH₄ is responsible for at least 25% of current global warming (Ocko et al.,
68 2021; Szopa et al., 2021). A 45% reduction in anthropogenic CH₄ emissions by 2030 would
69 avoid 0.25 °C in global warming by mid-century (Ocko et al., 2021), increasing the feasibility of
70 achieving the Paris Agreement goal.

71 CH₄ is emitted from a variety of anthropogenic and natural sources. Anthropogenic sources
72 account for 50–65% of total CH₄ emissions (Saunio et al., 2020), with approximately one third
73 of global anthropogenic CH₄ emissions originating from the fossil fuel-sector (i.e., emissions
74 from extraction, transport, processing of coal, oil and natural gas)(IEA, 2022). Although it is
75 important to tackle all sources of CH₄, emission reductions in the oil and gas (O&G) sector are
76 considered attractive, no-regret solutions. The International Energy Agency (IEA) estimates
77 that 75% of emissions reductions from the energy sector can be achieved at no net monetary
78 cost and could even result in economic savings, given that CH₄ is the main component of
79 natural gas and has commercial value (IEA, 2022). Thus, reducing CH₄ emissions from O&G
80 operations is one of the most substantial, easily accessible, and affordable mitigation actions
81 governments can take to address climate change.

82 Recent measurement-based studies in O&G production regions, mostly in North America,
83 have consistently shown that across years, scales, and methods, estimates of O&G CH₄
84 emissions often exceed emission inventory estimates (Zavala-Araiza et al. 2015; Shen et al.
85 2021; Gorchov Negron et al. 2020; Robertson et al. 2020; Alvarez et al. 2018; Tyner and
86 Johnson 2021; MacKay et al. 2021) with a few exceptions (e.g. Yacovitch et al. 2018; Foulds et
87 al. 2022). Inventory estimates tend to be based on outdated generic emission factors, which
88 may not reflect actual technologies and practices. Also, counts and location of facilities and
89 equipment used in inventories may be inaccurate or incomplete. Lastly, current inventories do
90 not capture the statistical characteristics of emission distributions that are found across the
91 O&G supply chain, which are usually heavy tailed and positively skewed (Alvarez et al., 2018;
92 Zavala-Araiza et al., 2017).

93 Romania is one of the oldest O&G producers in Europe with the first exploration dating
94 back to 1857. In 2021, Romania was the second largest oil producer and the largest natural
95 gas producer in the EU (BP, 2022). The recent gas discoveries in the Black Sea have the
96 potential to hold significant natural gas reserves, presenting an opportunity for the country to
97 enter a new phase of development. The EU announced an ambitious plan to urgently tackle
98 CH₄ emissions across all sectors by 2030 under the EU Methane Strategy (European
99 Commission, 2020). Underpinning this strategy, the EU recently announced draft regulations
100 for the oil and gas sector, focusing on robust measurement reporting and verification, leak
101 detection and repair, as well as minimizing venting and flaring (European Commission, 2021).
102 In the case of Romania, the uncertainty in current emission estimates and the lack of empirical
103 data makes the implementation of methane mitigation strategies challenging.

104 The Romanian Methane Emissions from Oil & Gas (ROMEIO) project aimed to address this
105 gap of knowledge (Röckmann, 2020). From September 30th to October 20th, 2019, a
106 measurement campaign took place in southern Romania with up to 70 participants from 14
107 research institutes. The goal of this project was to characterize CH₄ emissions at a component,
108 facility and basin scale using a variety of measurement platforms e.g., vehicles, Unmanned
109 Aerial Vehicles (UAVs), or commonly referred to as drones, and manned aircrafts. Through the
110 use of a range of emission quantification methods, the ROMEIO campaign aimed to provide a
111 comprehensive quantification of CH₄ emissions related to onshore O&G production in
112 Romania.

113 In this paper we analyse, integrate, and synthesize CH₄ emissions estimates collected by
114 vehicles and UAVs during the ROMEIO campaign, mainly focused on the characterization of oil
115 production sites. We (i) provide a comprehensive overview of the aggregated ground and
116 drone-based CH₄ emissions data, (ii) characterize the emission distributions and discuss the
117 differences between the quantification methods, (iii) present estimated emission factors
118 derived from the ground and drone-based measurements, (iv) identify major equipment
119 components of detected emissions across the O&G production sector, and (v) compare these
120 results to CH₄ emissions from emission inventories and production sites across other regions.

121 **2. Materials and methods**

122 **2.1. Investigated area**

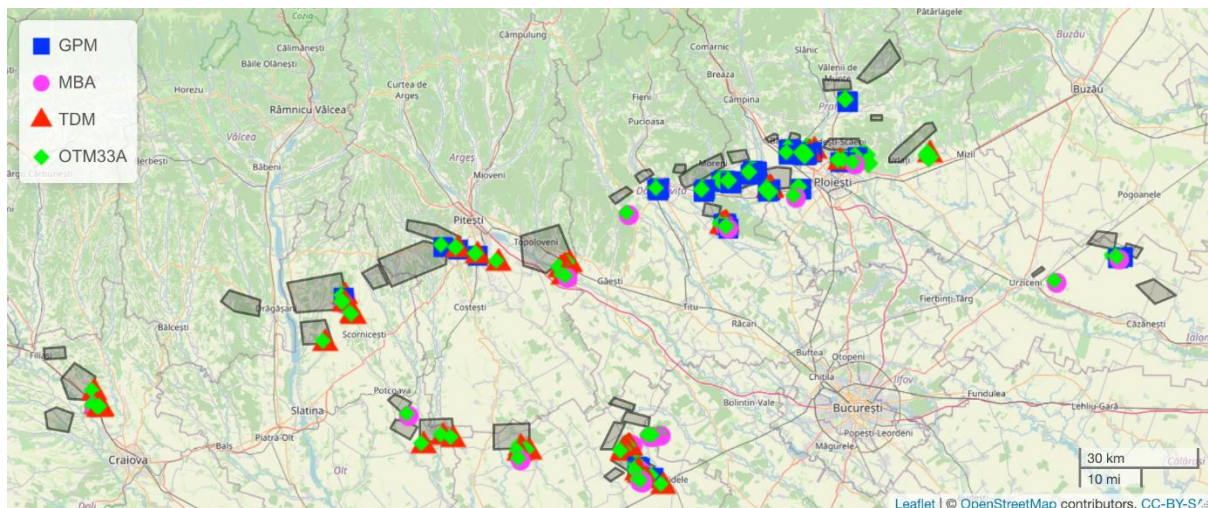
123 The 2019 ROMEIO campaign covered the southern part of Romania around the cities
124 Bucharest, Ploiesti, Pitesti, Targoviste and Craiova. Figure 1 shows that the O&G production
125 infrastructure is concentrated in smaller clusters that cover areas between 2 and 120 km²,
126 each containing 10 to 582 oil and gas related sites such as oil wells, gas wells, compressor
127 stations and oil parks. Different measurement teams visited different sites and clusters in
128 order to quantify as many O&G production sites as possible and to avoid a spatial sampling
129 bias. We note that most of the measurements presented here were individually described and
130 discussed in Delre et al. (2022) and Korbeń et al. (2022). Here we add the measurements
131 carried out from Unmanned Aerial Vehicle (UAV) platforms and integrate all ground and
132 drone-based data to perform upscaling emissions to the national scale.

133 The largest operator of O&G infrastructure in southern Romania, OMV-Petrom, provided a
134 list of production infrastructure coordinates and auxiliary information, such as type of
135 equipment, age, and for selected sites also production rate. Using this information, we
136 assessed the representativeness of our sampled sites in terms of production and age
137 characteristics (see S13 of Supplementary Material). A few additional emission points were
138 found that were not included in the infrastructure list provided by the operator. In these cases,

139 the site type was assigned based on visual inspection; in some cases, it could not be identified.
140 In our analysis we will combine the quantifications from all regions.

141 The majority of Romania's oil reservoirs are located in the southern part of the country.
142 With Romania producing about 3.3 million tonnes of oil in 2021 (BP, 2022), the southern region
143 is the most important part of the country's oil production sector. Most measurements during
144 the ROMEO campaign were collected from oil production sites, hence our analysis will focus
145 on this specific subset of sites. The oil production sites included in the study were usually
146 relatively simple, consisting of pump jacks and additional production equipment.

147



148

149 Figure 1. Map of the oil production sites that were quantified with four different measurement
150 approaches during the ROMEO campaign. The different symbols distinguish the different
151 quantification methods. Blue squares: Gaussian Plume Method (GPM); pink circles: Mass Balance
152 Approach (MBA); red triangles: Tracer Dispersion Method (TDM); green diamonds: Other Test
153 Method (OTM) - 33A. The grey shaded areas indicate clusters with high density of production facilities
154 (number of facilities ranging between 10 to 582), in some cases the symbols hide the areas.

155 2.2. Emission quantification

156 Facility scale measurements were divided into two phases: screening and quantification.
157 During the screening phase, the vehicles drove from site to site, circling the target site if
158 possible and recording CH₄ mole fractions above background. Screenings were performed
159 from public roads and the goal was to identify potential emissions at the site and check site
160 accessibility, considering factors such as roads condition, time limitations, and local
161 restrictions imposed by operators. To prevent any potential bias in the measured emissions,
162 the operators were not informed in advance about our visit to the facility, resulting in
163 occasional restricted site access. Additionally, the screenings aimed to determine whether off-
164 site sources such as other O&G infrastructure and farms, could interfere with subsequent
165 emission quantification, thereby ensuring the proper implementation of the quantification
166 methods. Also, a simplified Gaussian plume algorithm was applied for all locations where mole
167 fraction enhancements were observed to locate the sources based on the list of production
168 infrastructure provided by the operator, and to determine normalized CH₄ enhancements (see
169 S10 of Supplementary Material). A total of 1043 sites were screened using five cars. 85% of
170 these sites were oil production sites, and we focus on these for the following evaluation.

171 For quantification of CH₄ emission rates, four methods were used, namely the Tracer
172 Dispersion Method (TDM), Other Test Method (OTM) - 33A, Gaussian Plume Modelling (GPM)

173 using plume measurements from vehicles and Mass Balance Method (MBA) using Unmanned
174 Aerial Vehicle (UAV) based measurements (see S1). Here we provide a brief description of each
175 measurement method. Delre et al. (2022) provides additional information on the deployment
176 of TDM and GPM during the ROMEO campaign, while Korbeń et al. (2022) offers details
177 specifically on the deployment of OTM-33A and GPM.

178 The Tracer gas Dispersion Method (TDM) or tracer release method (Lamb et al. 1995) has
179 been widely used to quantify CH₄ emissions in the O&G sector (Allen et al., 2013; Zavala-Araiza
180 et al., 2018; Yacovitch et al., 2017; Roscioli et al., 2015). TDM involves the release of a tracer
181 gas at a controlled rate. When the tracer gas is released close to an emission point of the target
182 gas (CH₄), both gases undergo the same atmospheric transport processes. Therefore, even
183 when the plume dilutes, the ratio of their observed enhancements remains the same as the
184 ratio of their emission rates. Atmospheric concentrations of both the target gas and the tracer
185 gas can then be measured downwind to determine the unknown emission rate of the target
186 gas (CH₄). In this study, acetylene (C₂H₂) and nitrous oxide (N₂O) were used as tracer gases.

187 Two vehicles equipped with laser gas analysers were used to quantify CH₄ emissions with
188 the TDM. The first vehicle was equipped with two cavity ring-down spectroscopy analysers.
189 One instrument measured CH₄ (G2401, Picarro, Inc., Santa Clara, CA), and the other one
190 measured acetylene (C₂H₂) and nitrous oxide (N₂O) (S/N JADS2001, Picarro, Inc., Santa Clara,
191 CA). The second vehicle used a dual laser trace gas monitor based on Tunable Infrared Laser
192 Direct Absorption Spectroscopy to detect CH₄, C₂H₆, N₂O, CO₂, and CO simultaneously
193 (Aerodyne Research Inc., Billerica, MA). Measurements of CH₄ and tracer gases concentrations
194 were carried out by performing on average 9 downwind plume traverses. The site-
195 representative methane emission rate was then calculated by averaging the emission rates
196 estimated from the multiple traverses across the plume. A total of 50 quantifications were
197 performed at different sites using mobile and, in a few cases, static TDM.

198 The Gaussian plume method (GPM) uses an idealized calculation for the average local-scale
199 CH₄ dispersion, assuming constant meteorological conditions in time and space over a flat
200 region, to derive emission rate estimates from plume observations (Hanna et al. 1982). The
201 emission rate can then be calculated from measurements downwind of a source, using
202 information about the height of the source, wind speed and wind dispersion parameters
203 (Riddick et al., 2017). During the ROMEO campaign, multiple cars transects were carried out
204 downwind from the source at locations suitable for GPM. The emission rate for each location
205 was estimated based on the comparison between the results of the actual measured
206 concentrations and the results of the GPM. A total of 111 measurements were performed at
207 a variety of sites using GPM. GPM sub-sets from ROMEO have been investigated in Delre et al.
208 (2022) and Korbeń et al. (2022). In our analysis, we combine the GPM evaluation from the
209 different teams into one subset of emission quantifications.

210 Delre et al. (2022) compared emission rates derived from TDM and GPM evaluation
211 methods at 41 O&G sites. They found lower estimates from GPM evaluations compared to
212 TDM and applied a correction of a factor of 2 or more to the GPM quantifications (Delre et al.,
213 2022). We do not apply a correction to GPM measurements as done in Delre et al. (2022),
214 since a comparison to TDM is not possible for the other measurement teams (Korbeń et al.,
215 2022). Including the correction would lead to higher emission rate estimates. We also use a
216 different (parametric) statistical evaluation as described below.

217 Other Test Method (OTM) 33A is one of the Geospatial Measurement of Air Pollution
218 Remote Emission Quantification (GMAP-REQ) approaches developed by the United States
219 Environmental Protection Agency (EPA) (Thoma and Squier, 2014). This method uses
220 measurements with stationary analysers to detect and quantify emissions from a variety of

221 sources located near-field and at ground level (Robertson et al., 2020). Measurements were
222 performed by two vehicles equipped with in situ CH₄ analyzers. The first vehicle was equipped
223 with a high-precision Optical Feedback—Cavity-Enhanced Absorption Spectroscopy analyzer
224 (Licor Li-7810, LI-COR, Inc.) and detected CH₄ and CO₂ concentrations in ambient air. The
225 second vehicle was equipped with a cavity ring down spectrometer (CRDS, Model G1301,
226 Picarro Inc.). A total of 77 quantifications were performed at different sites using OTM-33A.

227 The Mass Balance Approach (MBA) has been applied widely to aircraft-based
228 measurements of CH₄ and other trace gases from the facility scale up to the basin scale (Karion
229 et al., 2013; O’Shea et al., 2014; Baray et al., 2018; Pitt et al., 2019). This method involves flying
230 at multiple heights downwind and/or around a region containing a possible emitting source
231 and measuring trace gas concentration and wind speed. Emission rates of the net surface flux
232 within that volume are then estimated from the difference between downwind and upwind
233 measurements (Morales et al., 2022).

234 Unmanned Aerial Vehicles (UAVs) are an emerging platform to investigate CH₄ emissions
235 from various sources such as landfills, dairy farms and natural gas compressor stations (Allen
236 et al., 2019; Vinković et al., 2022; Nathan et al., 2015; Andersen et al., 2018; Morales et al.,
237 2022; Shah et al., 2020; Shi et al., 2022). UAVs allow transecting the plume over its entire
238 vertical and horizontal extent, by flying at numerous heights, compared to ground-based
239 measurements that typically capture only part of the plume only at one height (Andersen et
240 al., 2018). Two different UAV-based systems were used to obtain atmospheric mole fraction
241 measurements downwind of oil and gas facilities during ROMEO: (i) an active AirCore system
242 from the University of Groningen (UG) (Vinković et al. 2022) and (ii) a lightweight fast-response
243 Quantum Cascade Laser Absorption Spectrometer (QCLAS) developed at the Swiss Federal
244 Institute for Materials Science and Technology (EMPA) (Tuzson et al., 2020; Morales et al.,
245 2022). A total of 125 flights (65 UG; 60 EMPA) were performed downwind of 43 different
246 facilities (19 UG; 24 EMPA). Both UAV-based techniques use an MBA to quantify the emission
247 rates from sampled oil and gas facilities, but there are certain differences in the MBA between
248 UG and EMPA application, including factors such as the treatment of wind, which are
249 presented in the supplementary material.

250 Several studies of CH₄ emissions from O&G infrastructure have found that emissions
251 distributions are typically heavy tailed and positively skewed with a small fraction of sites (i.e.,
252 super-emitters) accounting for a disproportionate fraction of emissions. These distributions
253 often become symmetric and normal when plotted as the logarithm of emissions. To account
254 for this behaviour, lognormal distributions have been widely used in the literature to more
255 accurately characterize emissions (Alvarez et al. 2018; Zavala-Araiza et al. 2015; 2017; 2018;
256 Robertson et al. 2020; Omara et al. 2016; Brandt et al. 2016; Yacovitch et al. 2017). We
257 examine whether our sampled data with emissions from oil production sites follow a
258 lognormal distribution by using two statistical tests (see S3). Table S2 of the supplemental
259 material shows that the null hypothesis of lognormality is accepted by both the Shapiro-Wilk
260 and Lilliefors test for all four measurement methods.

261 Several studies have evaluated site-level measurements from the O&G infrastructure using
262 non-parametric bootstrapping methods to derive emission factors (Rella et al., 2015; Brantley
263 et al., 2014; Robertson et al., 2017; Omara et al., 2016; Riddick et al., 2019). The previous
264 publications that evaluated subsets of the measurements reported here (Delre et al., 2022;
265 Korbeń et al., 2022) also used non-parametric approaches to estimate emission factors for a
266 systematic literature comparison. Non-parametric approaches typically derive EFs significantly
267 lower than the ones using parametric approaches. The parametric approaches take into
268 account the skewed distribution of the emission rates, particularly the disproportionate

269 contribution of emissions from the heavy tail of emission distributions. In particular, they
270 include the possibility that in the full distribution of sites, emission rates exist which are above
271 the maximum of the sampled subset. Therefore, parametric approaches and log-normal fits
272 have been used for up-scaling (Alvarez et al., 2018; Zavala-Araiza et al., 2015; Robertson et al.,
273 2020). As the emissions distribution in this work is highly positively skewed (see below), we
274 apply the parametric approach for scaling up to the total population of oil production sites in
275 Romania.

276 To this end, we calculate probability density functions (pdfs) of measured emission rates
277 that follow a log-normal distribution using Maximum Likelihood Estimation (MLE) (Zavala-
278 Araiza et al., 2015, 2018; Alvarez et al., 2018; Robertson et al., 2020). These pdfs are then used
279 to derive representative site-level Emission Factors (EF) which consider the low probability of
280 high-emission sites that describe skewed distributions. The mathematical formalism of this
281 statistical estimator is described in section S4 of the supplementary material, and we refer to
282 this approach as our reference method (A1).

283 The implementation of the log-normal fits requires information about the detection limit
284 of each method and the number of sites with emissions below this value (referred to as *non-*
285 *detects*). However, even when using the same analytical platform to measure emissions, the
286 lowest detectable emission rate will be affected by the distance between the emission point
287 and the analyser and by the meteorological conditions for a given measurement (Delre et al.,
288 2017). For our analysis, the detection limit for OTM-33A, GPM and MBA was empirically
289 determined equal to 0.11 kg h^{-1} and for TDM equal to 0.07 kg h^{-1} . Delre et al. (2022) and Korbeń
290 et al. (2022) determined the fraction of sites with emission rates below these detection limits
291 as 27% for TDM and 35% for OTM-33A, and GPM; the latter value is also adopted for MBA.

292 On the component scale, the combination of an Optical Gas Imaging (OGI) camera for the
293 detection of potential leak sources and a Hi-Flow Sampler (HFS) device for the quantification
294 of the emissions was implemented. A total number of 181 sites including 155 oil production
295 sites were visited and screened with a Forward-Looking InfraRed (FLIR) GasFindIR infrared
296 camera, the majority of them from the fence line. 231 individual leaks were detected with the
297 OGI camera but because of limited site access, the emission rates of only 62 leaking
298 components were measured using the HFS method. IR videos of the leaking components were
299 recorded to document detected emissions. These videos were reviewed to verify the number
300 of emission points and identify the type of emitting equipment.

301 From the OGI surveys we determined that a small but significant fraction of sites had no
302 emissions. While these surveys could potentially miss sources of emissions since they were
303 performed from the fence line (vs on-site), it allows us to derive a more conservative site-level
304 estimate, where we only add 1/3 of the non-detects to the main distribution of emitters. The
305 other 2/3 of the non-detects are considered as a separate mode of non-emitters with an EF of
306 0. These sites will also not be considered in the upscaling (see below). The final parameters
307 that are considered for the determination of the emission rate are provided in Table 2. A
308 detailed discussion on the determination of non-detects and the detection limits of the
309 different techniques is provided in sections S5 of the supplementary material. The effect of
310 the fraction of non-detects and the detection limit on the log-normal fits and the final EFs is
311 further explored by testing several different values (section S5). We find that reducing the
312 detection limit or increasing the fraction of non-detects leads to higher estimated EFs due to
313 the widening of the distribution towards the lower end. This emphasizes the importance and
314 need of conducting a thorough investigation when selecting the values for these two
315 parameters.

316 Additionally, in section S7 we present a sensitivity analysis with alternative upscaling
 317 approaches to explore upper and lower limits of the EF estimate for oil production sites. The
 318 main differences between these approaches are the choice of the detection limit and fraction
 319 of non-detects, the separation of the data into west and east regions and the separation by
 320 measurement method.

321 The combination of site-level emission estimates and component-level OGI surveys
 322 provided insights into the magnitude of emissions from oil production sites as well as key
 323 mitigation opportunities.

324

325 3. Results

326 3.1. Site-level quantifications of oil production sites

327 Approximately 887 oil production sites were screened, and emission rates were quantified
 328 from a total of 178 oil production sites. Table 1 provides basic statistics of the results obtained
 329 with the different measurement methods. The difference between the arithmetic mean and
 330 median estimates and the high positive values of skewness and kurtosis parameters
 331 demonstrate that the emission rates were positively skewed with a heavy tail for all methods.
 332 We find that the OTM-33A and GPM show the highest values of skewness and kurtosis,
 333 whereas the TDM and MBA present the least skewed and heavy tailed distributions. Figure 2
 334 illustrates the boxplots of the distributions of the quantified emission rates per method. It is
 335 important to note that the sampled oil production sites are different for each method (and
 336 sampled at different points in time), thus Figure 2 summarizes the sampled emissions
 337 distributions and the observed differences in Figure 2 may be influenced by factors such as
 338 variations in emissions magnitude and variability at each specific oil production site.

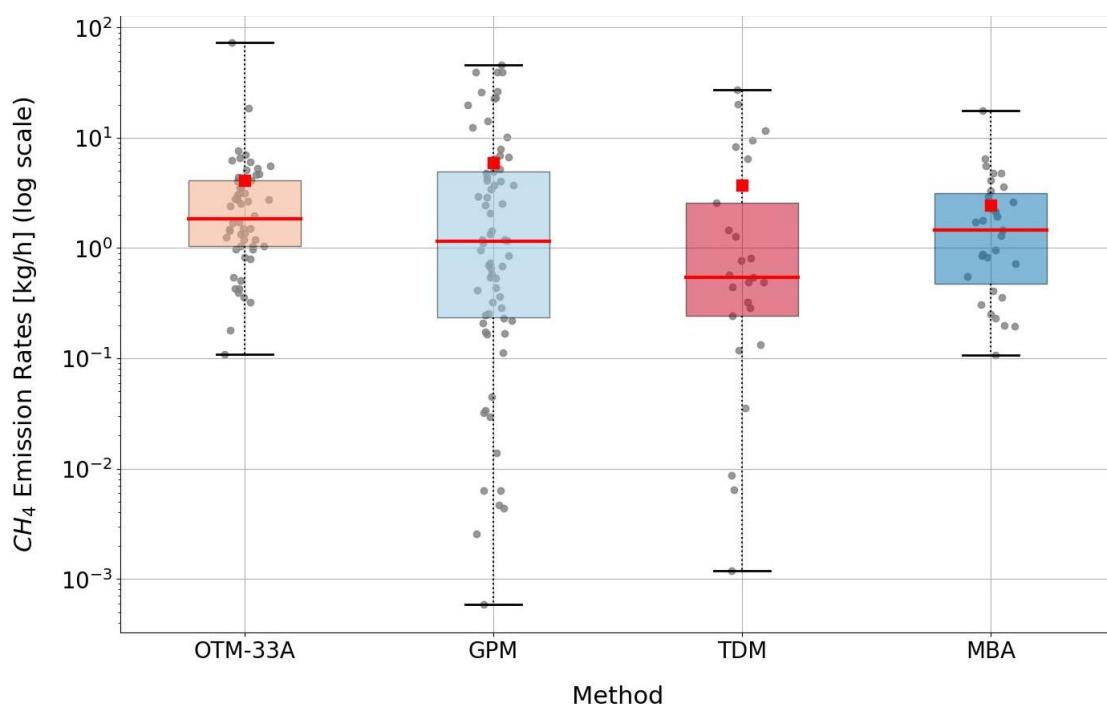
339 Table 1. Basic statistics of measured CH₄ emission rates by method.

Method	# Oil production sites	Arithmetic mean [kg h ⁻¹]	Median [kg h ⁻¹]	Min [kg h ⁻¹]	Max [kg h ⁻¹]	Skew ^b	Kurtosis ^c
OTM-33A	54	4.1	1.9	0.1100	73	6.3	40
GPM ^a	68	6.1	1.0	0.0006	118	5.4	34
TDM	25	3.7	0.5	0.0012	27	2.3	4
MBA	31	2.4	1.5	0.1100	18	3.3	12

340 ^aIncluding the oil production sites evaluated as "Estimate" in Delre et al. (2022) using only one
 341 concentration record (see S2)

342 ^bSkewness is a measure of the asymmetry of a data distribution. Skewness of zero represents a normal
 343 distribution. Positive (negative) values indicate that the data is positively (negatively) skewed.

344 ^cKurtosis is a measure indicating whether the data distribution is heavy-tailed or light-tailed relative to
 345 a normal distribution. Kurtosis of zero represents a normal distribution. Positive (negative) kurtosis
 346 indicates a "heavy-tailed" ("light-tailed") distribution.



347
 348 Figure 2. Boxplots of the distributions of quantified emission rates from oil production sites per
 349 method. In each box the red horizontal line signifies the median and the red squares show the mean.
 350 The box extends to the 25th and 75th percentiles. The whiskers extend from the minimum to the
 351 maximum value. The data points are overlaid on top of the boxplots (grey dots). Note the logarithmic
 352 y-axis.

353 3.2. Emissions distributions and emission factors

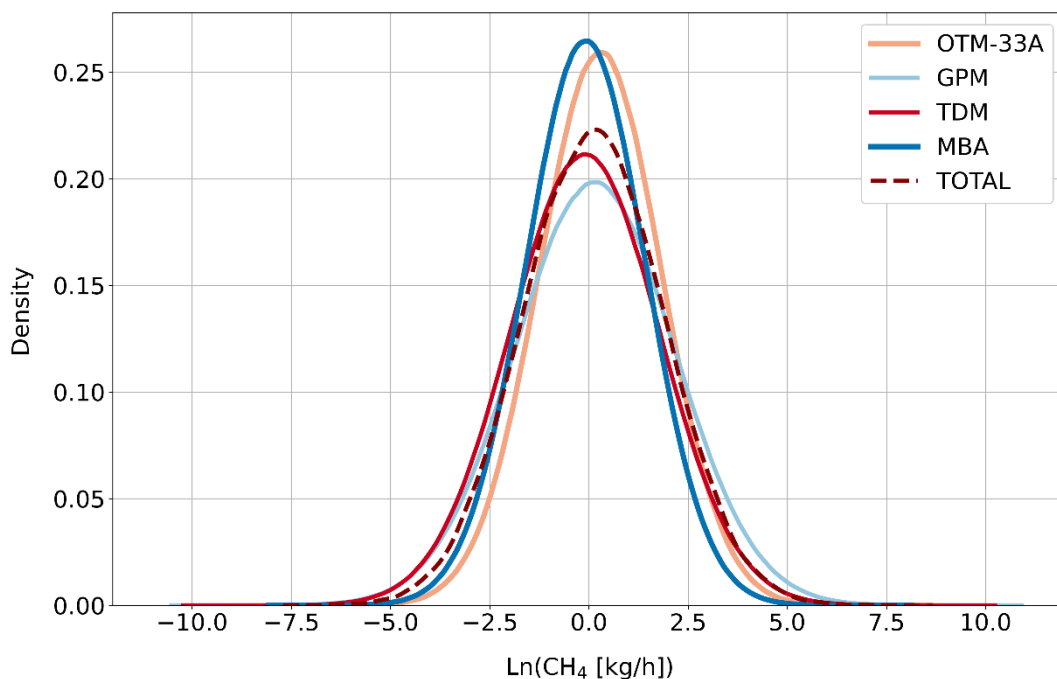
354 Figure 3 shows the pdfs generated from fitting the quantified emission rates to lognormal
 355 distributions. In Table 2 we summarize key parameters and derived EFs that characterize these
 356 distributions. Across methods, best estimates for EFs range from 2.9 – 8.8 kg h⁻¹ of CH₄ site⁻¹.
 357 The pdf of GPM shows the widest distribution and a large confidence interval (CI). The effect
 358 of the small sample size is reflected in the large 95% CI of TDM relative to the other methods.
 359 When we combine all the quantifications (solving for one single Maximum Likelihood
 360 Estimation, see SM) we obtain a central estimate of mean site-level emission equal to 5.4 kg
 361 h⁻¹ of CH₄ site⁻¹ (3.6 – 8.4, 95% CI). For information, histograms and fitted pdfs for each method
 362 used are shown in Fig. S7 of the SM.

363
 364 Table 2. Summary of parameters from the statistical estimator.

Method	DL [kg h ⁻¹]	S _r	S _o [% of non-detects]	μ	σ	EF [kg h ⁻¹ site ⁻¹]	95% CI
OTM-33A	0.11	53	7 [12%]	0.28	1.54	4.3	2.4 – 8.2
GPM	0.11	57	8 [12%]	0.15	2.01	8.8	3.7 – 23
TDM	0.07	21	2 [9%]	-0.10	1.89	5.4	1.6 – 23
MBA	0.11	30	4 [12%]	-0.08	1.51	2.9	1.4 – 6.6
TOTAL	-	-	-	0.12	1.77	5.4	3.6 – 8.4

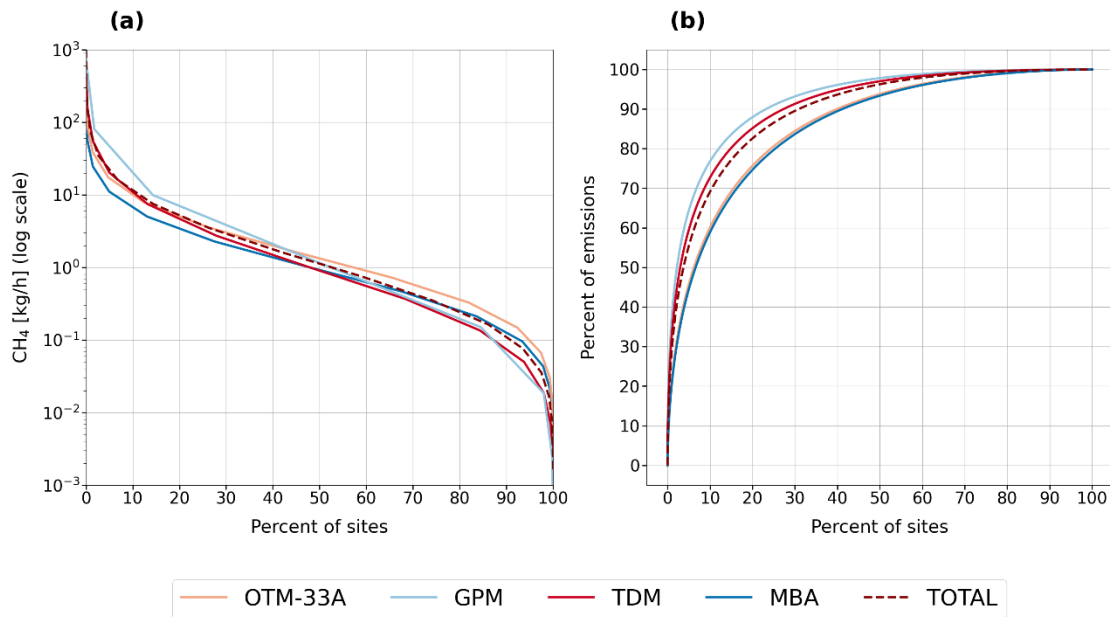
365 DL is the assigned detection limit for each measurement method, S_r is the number of measurements
 366 above the detection limit, S_o is the number of measurements at or below the detection limit (included
 367 as censored data). Note that in actual measurements even emission rates below this limit are

368 sometimes detected (see Fig. 2). In our statistical approach these measurements are replaced by the
 369 fraction of non-detects S_0 . Therefore, the numbers for S_r are different the total number of oil
 370 production sites visited given in Table 1. $EF = e^{\mu + \frac{1}{2}\sigma^2}$, TOTAL
 371 presents the results of the statistical estimator considering all four measurement methods.



372
 373 Figure 3. Fitted pdfs of the statistical estimator for each measurement method.

374 The cumulative distribution functions and Lorenz curves from all measurement methods
 375 using the statistical estimator (Fig. 4) verify once more that the distributions are highly skewed.
 376 For the quantified population of oil production sites, we find that 10% of emitters had
 377 emissions greater than 10 kg h^{-1} and were responsible for over 70% of total emissions. The
 378 estimates from the different methods reflect the qualitative illustration in Fig. 3: The results
 379 obtained with GPM show the most skewed distribution with the 10% of oil production sites
 380 with highest emissions contributing to 77% of total emissions, whereas for the oil production
 381 sites measured with the MBA 60% of cumulative CH_4 emissions are attributed to 10% of oil
 382 production sites.



383

384 Figure 4. a) Cumulative distribution functions, b) Lorenz curves: percent of emissions as a function
 385 of percent of sites. For both graphs, oil production sites are sorted from high to low emission rates
 386 (descending order).

387 In the supplementary material (sections S7) we provide additional estimates of the total
 388 CH₄ basin EFs calculated using modifications of the reference statistical approach in order to
 389 explore the sensitivity to the chosen parameters. By using the same reference approach and
 390 including a higher fraction non-detects, ranging between 27 – 35%, the derived EF is 53%
 391 higher. Compared to the EF calculated with the reference approach, the EFs calculated using
 392 the alternative approaches are between 35 –83% higher. All of these estimates agree within
 393 the ranges of uncertainty, confirming that the high EFs are not due to details of the statistical
 394 treatment. For comparison of our values to other studies (see below) we use the Ref scenario
 395 (A1) discussed in the previous sections which is our lowest and most conservative estimate
 396 and includes a separate mode of non-emitters (zero mode) and a correspondingly lower
 397 fraction of non-detects for the main mode of emitters (9 - 12%).

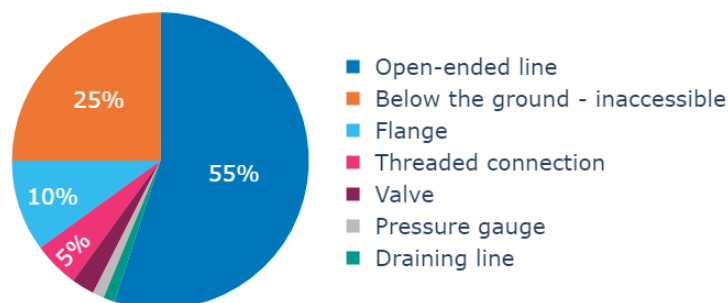
398

399 3.3. Identification of leaking components

400 By using the recorded videos of the leaking components, emission sources could be
 401 attributed to specific major equipment types across the O&G production sector. A total of 155
 402 oil production sites were screened with the infrared camera, corresponding to approximately
 403 3% of the total population of oil production sites provided by the operator. CH₄ emissions were
 404 detected from approximately half (49%) of these sites. At least one leak was detected at 74
 405 out of the 155 screened oil production sites with an average of 1.2 leaks detected per site. A
 406 total of 86 individual leaks were identified at the oil production sites. The HFS method was
 407 used to measure emissions from a small subset of leaks (i.e., when access to the leaky
 408 component was possible), results are summarized in the SM (see S11) but were not used as
 409 part of the main analysis since they do not represent a complete assessment of the magnitude
 410 of emissions.

411 Figure 5 shows the distribution of the identified leaking components for oil production
 412 sites. The most frequently detected sources were open-ended lines, accounting for more than
 413 half (55%) of the detected components. An open-ended line refers to a pipe or tubing that is

414 not sealed at one end, and therefore remains open to the atmosphere, allowing all gas to be
 415 vented to the atmosphere. Following open-ended lines, inaccessible components located
 416 below the ground comprised 25% of the detected sources, while malfunctioning equipment
 417 such as flanges and threaded connections accounted for 20%. It should be noted that the
 418 inaccessible and, as a result, non-identified components below the ground may consist of
 419 valves, pumps, connectors, or potentially open-ended lines.



420

421 Figure 5. Frequency of identified leaking components for oil production sites (n = 86).
 422

423

3.4. Other types of facilities

424 In addition to oil production sites, we visited also other types of infrastructure (gas
 425 production sites, oil parks, compressor stations, etc) during the ROMEO campaign. Due to the
 426 low number of quantifications for these types of infrastructure, a statistically robust
 427 quantitative evaluation is impossible, but we provide here some qualitative information. The
 428 largest emission rates were observed from an oil park with 138 kg/h, while the average
 429 emission rate from 17 oil parks was 17 kg/h. An oil park is a facility designed to gather, store,
 430 and distribute oil produced from multiple individual wells in the surrounding area. The most
 431 important sources of CH₄ emissions from oil parks were leaks in storage tanks and other
 432 malfunctioning equipment, such as valves or flanges. We visited two compressor stations and
 433 found 58 and 27 leaks, approximately half of them were quickly repaired in one day by the
 434 technicians from the operator. The complete list of all quantifications is provided in section
 435 S14 of the SM.

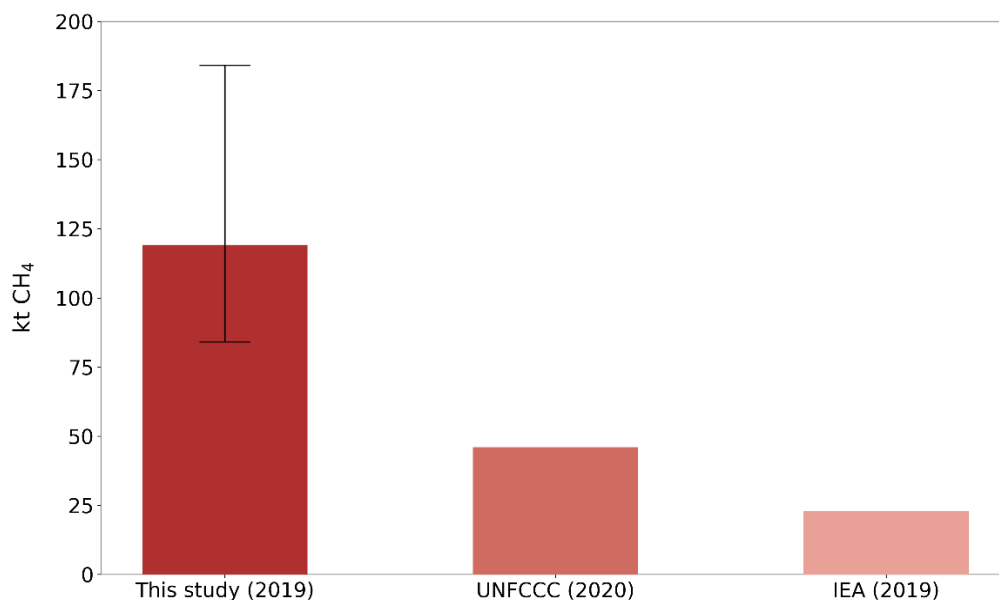
4. Discussion

437 To compare our results with the reported emissions from national inventories, we assume
 438 that the measured oil production sites in this study are representative of oil production sites
 439 basin-wide. We scale up our emissions to the country level by using our central estimate of
 440 5.4 kg h⁻¹ site⁻¹ for the evaluation including a separate mode of no-emitters, as explained
 441 above. This leads to an activity factor of N ≈ 2500 for the year 2019. Assuming that these
 442 emissions continue year-round, this results in annual emission estimate of 120 ktons CH₄ (min
 443 = 79 ktons and max = 180 ktons, 95% CI).

444 In Fig. 6, our measurement-based estimates are compared to inventory reports. Methane
 445 emissions from Romania for the year 2020 reported to the United Nations Framework
 446 Convention on Climate Change (UNFCCC) in category 1.B.2.a (CH₄ from Oil, sub-categories i:
 447 exploration and ii: production) and category 1.B.2.c (Venting and Flaring) sum up to 46 ktons
 448 of CH₄ (Greenhouse Gas Inventory Data - Comparison by Category, 2022). The IEA estimate for

449 Romanian emissions from the categories *Onshore Oil* and *Other from oil and gas* for the year
 450 2019 is 23 ktons of CH₄ (Methane Tracker Data Explorer, 2022). Thus, the emission rates
 451 derived in our study are approximately 2.5 times higher than the UNFCCC inventory and more
 452 than 5 times higher than the IEA estimate. Note that our reference statistical approach is a
 453 conservative one as shown in the sensitivity study in the SM. Our estimates also only include
 454 producing oil production sites, and not even the total population of oil production sites in
 455 Romania. Documented emissions from other types of sites, e.g., oil parks with our
 456 documented emissions from leaking tanks, and the entire gas production infrastructure, were
 457 not included. Non-producing oil production sites were also neglected for the derivation of
 458 country-level annual emissions, although emissions were still detected from nine oil
 459 production sites that were characterised as non-operating by the operator.

460 The total emission rate from all oil production sites that were quantified in this study was
 461 810 kg/h whereas the sum of quantifications of all types of infrastructure visited during the
 462 ROMEO campaign was 2100 kg/h. Although we do not have a sufficient statistical basis for a
 463 thorough quantification of other types of infrastructure, this indicates that the total CH₄
 464 emissions from the O&G infrastructure in Romania could be at least a factor 2 higher than our
 465 estimate from oil production sites.



466 Figure 6. Comparison of annual CH₄ emissions estimated in our study for 2019 with emissions
 467 reported to the UNFCCC in category 1.B.2.a (CH₄ from Oil, sub-categories *i*: exploration and *ii*:
 468 production) and category 1.B.2.c (Venting and Flaring) for the year 2020 and derived by the IEA for
 469 categories *Onshore Oil* and *Other from oil and gas* for the year 2019. Error bar extends from the lower
 470 bound (i.e., 79 ktons yr⁻¹) to the upper bound (i.e., 180 ktons yr⁻¹) of the 95% CI.
 471

472 Discrepancies between available inventory estimates and direct measured CH₄ emissions
 473 have been indicated by numerous studies in other areas (Robertson et al., 2020; MacKay et
 474 al., 2021; Alvarez et al., 2018; Zavala-Araiza et al., 2015; Tyner and Johnson, 2021; Rutherford
 475 et al., 2021), and we now confirm this discrepancy is large for Romania. One reason for these
 476 discrepancies is the use of outdated and highly uncertain EFs for the derivation of inventory
 477 estimates. This is especially relevant for Romania since their published estimates are based on
 478 the basic Tier 1 method, which relies on multiplying default EF applicable for all countries by

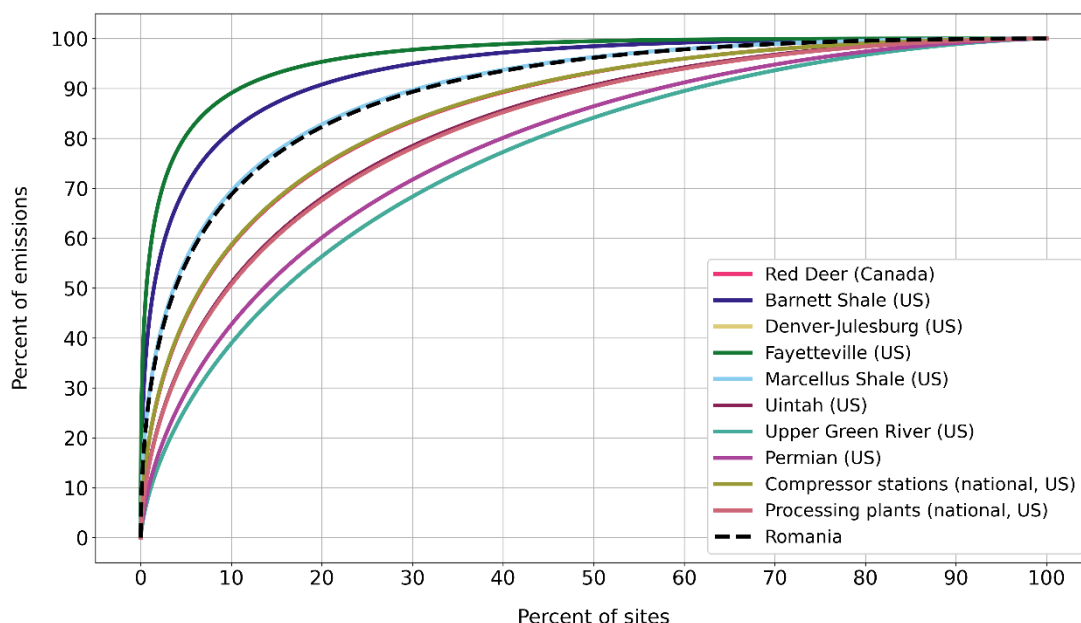
479 country-specific activity data following the IPCC 2006 guidelines (Eggleston et al., 2006). Thus,
 480 these reported emissions do not consider the characteristics of the actual O&G infrastructure
 481 of Romania, such as its age and state of maintenance, or current operational practises. For
 482 example, emission reduction by gas flaring has been almost eliminated as a practice in
 483 Romania. Additionally, infrastructure for the collection and economical utilization of the
 484 natural gas that would otherwise be flared or vented is inadequate or non-existing in the
 485 sampled areas, as illustrated by the high fraction of surveyed sites, where direct venting was
 486 the main source of emission.

487 To place the results from the ROME campaign in perspective, we compare them to studies
 488 performed in O&G production areas in the US and Canada (Robertson et al., 2020, 2017;
 489 Zavala-Araiza et al., 2015, 2018; Omara et al., 2016). We use the reported datasets from these
 490 studies to derive the EFs using the statistical approach used in this paper. In this way we
 491 eliminate inconsistencies from data treatment and can consistently compare the results
 492 between the different regions.

493 The CH₄ EF estimated for Romania is 5.4 kg h⁻¹ site⁻¹ (3.6 – 8.4, 95% CI). EFs estimated for
 494 the studies used for our comparison range between 1.2 and 8.2 kg h⁻¹ site⁻¹ for O&G
 495 production sites (e.g., oil well and/or gas well sites), with the majority of the EFs being below
 496 3 kg h⁻¹ site⁻¹ (see Table S13). Specifically, our estimated CH₄ EF from Romania is the third
 497 highest EF calculated from a variety of production regions in North America. The differences
 498 between production characteristics, age of sites, geologic features and operational procedures
 499 in each region could have a significant impact on the various levels of skewness and the EFs.

500 Figure 7 shows the derived cumulative distribution functions of each production region. All
 501 studies show heavy-tailed distributions; however, Romania presents the fourth highest level
 502 of skewness indicating the disproportionate contribution of high-emitting sites to the total
 503 emissions. Our results show that 10% of sites are responsible for more than 70% of emissions.
 504 By identifying and mitigating these high-emitting sites or "super-emitters", a large share of
 505 total emissions reduction can be achieved.

506

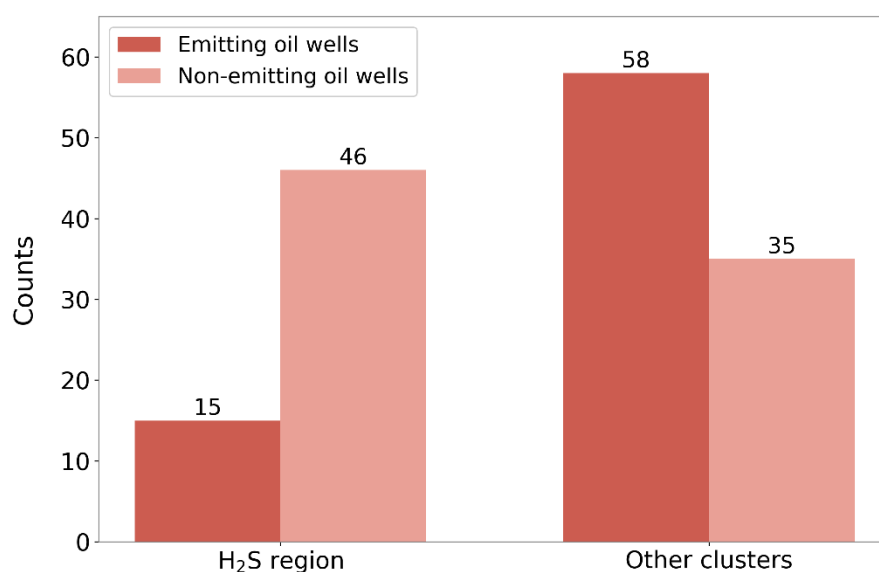


507
 508 Figure 7. Lorenz curve: cumulative percentage of emissions as a function of cumulative percentage of
 509 sites (sorted from high to low emissions) for different North American production regions, including
 510 the results from this study. The black dashed line shows the results of the statistical estimator for the

511 ROMEO campaign, considering all four measurement methods. It overlaps with the one from the
512 Marcellus Shale basin. Red deer line overlaps with compressor stations line, and Uintah line overlaps
513 with processing plants line.

514 On the component scale, 55% of emission points from oil production sites are from open-
515 ended lines and another 25% from non-identified components below the ground, which are
516 possibly open outlets as well. These vents are thus part of the operational practices and can
517 be avoided by prioritizing gas capture infrastructure.

518 An important finding of the OGI dataset analysis is the much lower percentage of emitting
519 oil production sites in a production cluster, where the produced oil is associated with
520 emissions of Hydrogen Sulfide (H₂S) gas (Fig. 8). H₂S is a by-product that is formed in some
521 fossil fuel reservoirs through natural processes or due to some methods employed in the O&G
522 upstream production (Marriott et al., 2016). It is highly toxic to humans and animals, causing
523 serious health problems even at low concentrations (Doujaiji and Al, 2010). The lower fraction
524 of emitting oil production sites in this cluster indicates that sites associated with the H₂S
525 component are better maintained to avoid harmful H₂S emissions. This demonstrates that it
526 is feasible to reduce emissions by improved practises and better maintenance of facilities.
527 These findings are consistent with the research conducted by Lavoie et al. (2022), which
528 showed that reduction strategies focusing on olfactory compounds in Peace River have proven
529 beneficial in reducing and maintaining lower CH₄ emissions, despite not being specifically
530 designed for CH₄ reduction purposes (Lavoie et al., 2022). However, it is important to note
531 that further research is needed to establish a clear relationship between CH₄ and H₂S emission
532 rates.



533 Figure 8. Number of screened oil production sites, divided by sites with identified leaks and sites
534 without identified leaks, from the H₂S region in comparison to other clusters.
535

536 An independent line of evidence for large scale venting in Romania is that 70% of the
537 screened oil production sites and more than 50% of measured oil production sites are listed
538 with zero gas production in the database of the operator. Evidently, when associated gas is
539 vented via open vents immediately at the well head, it will not be metered and thus cannot
540 be quantified and reported.

541 Our results have great implications not only for the accuracy of current national inventories,
542 but also for the feasibility of reaching EU emissions reductions targets. The total CH₄ emissions
543 from the O&G sector in Romania reported to the UNFCCC decreased by 93% between 1989
544 and 2020 (Greenhouse Gas Inventory Data - Comparison by Category, 2022). However, this
545 significant reduction is primarily due to the change of the TIER 1 emission factor from the one
546 for developing countries to the one for developed countries in the year 2000. It is a
547 consequence of decrease in production and changes in reporting methodology, and not
548 indicative of changes in operations that would result in lower emissions. The lack of gas flaring
549 and gas collection infrastructure across oil production sites in Romania is evidence of the
550 relatively high emissions. Additionally, a large number of countries rely on the Tier 1 method,
551 rather than direct site-level measurements, for the derivation of their national emissions
552 estimates from the energy sector. However, since technological and operating conditions vary
553 significantly between countries, these estimates are associated with large uncertainties and
554 might not reflect actual emissions.

555 Our work highlights the need for better understanding of the level of emissions in the O&G
556 industry. Due to the significant regional differences in age, site design, and operational
557 practices, the O&G production region in one country, such as southern Romania, may not be
558 representative of other production regions around the world. Therefore, emission factor
559 estimates, and mitigation options cannot be generalised. Our work, however, illustrates how
560 empirical data collected at both facility and component scales can significantly reduce the
561 uncertainty in the magnitude of emissions and identify key mitigation opportunities specific
562 to a country's local conditions.

563

564 **5. Conclusions**

565 In this work, we provide a thorough characterization of CH₄ emissions from oil production
566 sites in Romania by integrating a variety of ground and drone-based quantification methods.
567 The main findings are summarized as follows:

- 568 1. Emission rates from oil production sites were represented by a mean EF equal to 5.4 kg
569 h⁻¹ site⁻¹ (3.6—8.4, 95% CI). The derived EF for Romania is one of the highest EFs found
570 in previous studies.
- 571 2. The CH₄ emission rate distribution is highly skewed, with 10% of sites contributing to
572 more than 70% of the total CH₄ emissions.
- 573 3. Oil production sites associated with emissions of H₂S are better maintained and had a
574 lower number of detected emission points compared to oil production sites without H₂S
575 emissions. Thus, effective mitigation of emissions can be achieved by improved practices.
- 576 4. The Romanian national inventory underestimates O&G CH₄ emissions by at least a factor
577 of 2, likely more. Given the importance of mitigating CH₄ emissions in the near-term
578 future, and the ambitious mitigation targets announced by governments and industry,
579 improvement of emission reporting based on measurements is key to track changes in
580 emissions over time.
- 581 5. Major drivers of CH₄ emissions from oil production sites in Romania are the venting of
582 gas through open-ended lines followed by technical malfunctioning equipment.
- 583 6. Our results highlight significant opportunities for emission mitigation. Development of
584 infrastructure for the capture and utilization of natural gas combined with replacement

585 and upgrade of equipment would address the primary sources of Romanian O&G
586 emissions. Further reductions can be achieved by identifying and repairing equipment
587 leaks through frequent monitoring of methane emissions and implementation of leak
588 detection and repair programs. Focusing on these mitigation actions would be an
589 effective and efficient strategy to achieve substantial methane reductions.

590

591 **Data availability**

592 The emission rates dataset used in this study is presented in Table S16 in the Supplementary
593 Material.

594

595 **Author contributions**

596 Study design: TR, HC, MS, JMN, AnC

597

598 Execution and planning of ground and drone based measurements: KV, BK, MdV, SvH, PK, MS,
599 JW, PJ, JMN, JB, HM, MM, CvdV, BT, JR, RPM, LE, DB, MS, AH, IV, PvdB, HDvdG, AD, MEE, CS,
600 MC, SI, DM, AS, AT, IV, AnC, MA, SG, AP, AuC, LC, AN, CB, CP, AR, AM, HS, BH, SS, DZA, HC, TR

601

602 Data evaluation: FS, KV, PK, MS, PJ, JMN, JB, HM, BT, JR, RPM, LE, AH, IV, HDvdG, AD, CS, AnC,
603 SS, DZA, HC, TR

604

605 Preparation of manuscript: FS, DZA, KV, HC, TR with input from PK, MS, PJ, JMN, JB, HM, BT,
606 LE, AH, IV, HDvdG, AD, CS, AnC, SS

607

608 **Acknowledgements**

609 Our collected data, funded by UNEP's International Methane Emissions Observatory (IMEO) is
610 part of a science studies programme that aims to support methane emission mitigation
611 strategies, actions and policies.

612

613 **Funding**

614 The Romanian Methane Emission from Oil & Gas (ROME) campaign was initiated and largely
615 carried out by participants of the European H2020 project MEMO² (MEthane goes MOBILE -
616 MEasurements and Modelling), which was funded by the European Union's Horizon 2020
617 research and innovation programme under the Marie Skłodowska-Curie grant agreement No.
618 722479. Additional funding was provided by the Climate and Clean Air Coalition (CCAC) Oil &
619 Gas Methane Science Studies (MSS), administered through United Nations Environment
620 Programme (UNEP) under grant number PCA/ CCAC/UU/DTIE19-EN652.

621

622 **Competing interests**

623 The authors declare that they have no conflict of interest.

624

625 **References**

626 Allen, D. T., Torres, V. M., Thomas, J., Sullivan, D. W., Harrison, M., Hendler, A., Herndon, S. C., Kolb, C. E., Fraser,
627 M. P., Hill, A. D., Lamb, B. K., Miskimins, J., Sawyer, R. F., and Seinfeld, J. H.: Measurements of methane emissions
628 at natural gas production sites in the United States, Proc. Natl. Acad. Sci., 110, 17768–17773,
629 <https://doi.org/10.1073/pnas.1304880110>, 2013.

630 Allen, G., Hollingsworth, P., Kabbabe, K., Pitt, J. R., Mead, M. I., Illingworth, S., Roberts, G., Bourn, M., Shallcross,
631 D. E., and Percival, C. J.: The development and trial of an unmanned aerial system for the measurement of
632 methane flux from landfill and greenhouse gas emission hotspots, *Waste Manag.*, 87, 883–892,
633 <https://doi.org/10.1016/j.wasman.2017.12.024>, 2019.

634 Alvarez, R. A., Zavala-Araiza, D., Lyon, D. R., Allen, D. T., Barkley, Z. R., Brandt, A. R., Davis, K. J., Herndon, S. C.,
635 Jacob, D. J., Karion, A., Kort, E. A., Lamb, B. K., Lauvaux, T., Maasakkers, J. D., Marchese, A. J., Omara, M., Pacala,
636 S. W., Peischl, J., Robinson, A. L., Shepson, P. B., Sweeney, C., Townsend-Small, A., Wofsy, S. C., and Hamburg, S.
637 P.: Assessment of methane emissions from the U.S. oil and gas supply chain, *Science*, 361, 186–188,
638 <https://doi.org/10.1126/science.aar7204>, 2018.

639 Andersen, T., Scheeren, B., Peters, W., and Chen, H.: A UAV-based active AirCore system for measurements of
640 greenhouse gases, *Atmospheric Meas. Tech.*, 11, 2683–2699, <https://doi.org/10.5194/amt-11-2683-2018>, 2018.

641 Baray, S., Darlington, A., Gordon, M., Hayden, K. L., Leithead, A., Li, S.-M., Liu, P. S. K., Mittermeier, R. L., Moussa,
642 S. G., O'Brien, J., Staebler, R., Wolde, M., Worthy, D., and McLaren, R.: Quantification of methane sources in the
643 Athabasca Oil Sands Region of Alberta by aircraft mass balance, *Atmospheric Chem. Phys.*, 18, 7361–7378,
644 <https://doi.org/10.5194/acp-18-7361-2018>, 2018.

645 BP: Statistical Review of World Energy 2022 (71st edition), BP, 2022.

646 Brandt, A. R., Heath, G. A., and Cooley, D.: Methane Leaks from Natural Gas Systems Follow Extreme
647 Distributions, *Environ. Sci. Technol.*, 50, 12512–12520, <https://doi.org/10.1021/acs.est.6b04303>, 2016.

648 Brantley, H. L., Thoma, E. D., Squier, W. C., Guven, B. B., and Lyon, D.: Assessment of Methane Emissions from
649 Oil and Gas Production Pads using Mobile Measurements, *Environ. Sci. Technol.*, 48, 14508–14515,
650 <https://doi.org/10.1021/es503070q>, 2014.

651 Delre, A., Mønster, J., and Scheutz, C.: Greenhouse gas emission quantification from wastewater treatment
652 plants, using a tracer gas dispersion method, *Sci. Total Environ.*, 605–606, 258–268,
653 <https://doi.org/10.1016/j.scitotenv.2017.06.177>, 2017.

654 Delre, A., Hensen, A., Velzeboer, I., van den Bulk, P., Edjabou, M. E., and Scheutz, C.: Methane and ethane
655 emission quantifications from onshore oil and gas sites in Romania, using a tracer gas dispersion method, *Elem.
656 Sci. Anthr.*, 10, 000111, <https://doi.org/10.1525/elementa.2021.000111>, 2022.

657 Doujaiji, B. and Al, -Tawfiq Jaffar A.: Hydrogen sulfide exposure in an adult male, *Ann. Saudi Med.*, 30, 76–80,
658 <https://doi.org/10.4103/0256-4947.59379>, 2010.

659 Eggleston, H. S., Buendia, L., Miwa, K., Ngara, T., and Tanabe, K.: 2006 IPCC Guidelines for National Greenhouse
660 Gas Inventories, 2006.

661 European Commission: COMMUNICATION FROM THE COMMISSION TO THE EUROPEAN PARLIAMENT, THE
662 COUNCIL, THE EUROPEAN ECONOMIC AND SOCIAL COMMITTEE AND THE COMMITTEE OF THE REGIONS on an
663 EU strategy to reduce methane emissions, 2020.

664 European Commission: Proposal for a REGULATION OF THE EUROPEAN PARLIAMENT AND OF THE COUNCIL on
665 methane emissions reduction in the energy sector and amending Regulation (EU) 2019/942, 2021.

666 Foulds, A., Allen, G., Shaw, J. T., Bateson, P., Barker, P. A., Huang, L., Pitt, J. R., Lee, J. D., Wilde, S. E., Dominutti,
667 P., Purvis, R. M., Lowry, D., France, J. L., Fisher, R. E., Fiehn, A., Pühl, M., Bauguitte, S. J. B., Conley, S. A., Smith,
668 M. L., Lachlan-Cope, T., Pisso, I., and Schwietzke, S.: Quantification and assessment of methane emissions from
669 offshore oil and gas facilities on the Norwegian Continental Shelf, *Atmospheric Chem. Phys.*,
670 <https://doi.org/10.5194/acp-2021-872>, 2022.

671 Gorchoy Negron, A. M., Kort, E. A., Conley, S. A., and Smith, M. L.: Airborne Assessment of Methane Emissions
672 from Offshore Platforms in the U.S. Gulf of Mexico, *Environ. Sci. Technol.*, 54, 5112–5120,
673 <https://doi.org/10.1021/acs.est.0c00179>, 2020.

674 Hanna, S. R., Briggs, G. A., and Hosker, J.: Handbook on atmospheric diffusion, National Oceanic and Atmospheric
675 Administration, Oak Ridge, TN (USA). Atmospheric Turbulence and Diffusion Lab.,
676 <https://doi.org/10.2172/5591108>, 1982.

677 IEA: <https://www.iea.org/reports/global-methane-tracker-2022>, last access: 2 November 2022.

678 Methane Tracker Data Explorer: <https://www.iea.org/data-and-statistics/data-tools/methane-tracker-data-explorer>, last access: 2 November 2022.

680 Karion, A., Sweeney, C., Pétron, G., Frost, G., Michael Hardesty, R., Kofler, J., Miller, B. R., Newberger, T., Wolter,
681 S., Banta, R., Brewer, A., Dlugokencky, E., Lang, P., Montzka, S. A., Schnell, R., Tans, P., Trainer, M., Zamora, R.,
682 and Conley, S.: Methane emissions estimate from airborne measurements over a western United States natural
683 gas field, *Geophys. Res. Lett.*, 40, 4393–4397, <https://doi.org/10.1002/grl.50811>, 2013.

684 Korbeń, P., Jagoda, P., Maazallahi, H., Kammerer, J., Nećki, J. M., Wietzel, J. B., Bartyzel, J., Radovici, A., Zavala-
685 Araiza, D., Röckmann, T., and Schmidt, M.: Quantification of methane emission rate from oil and gas wells in
686 Romania using ground-based measurement techniques, *Elem. Sci. Anthr.*, 10, 00070,
687 <https://doi.org/10.1525/elementa.2022.00070>, 2022.

688 Lamb, B. K., McManus, J. B., Shorter, J. H., Kolb, C. E., Mosher, Byard., Harriss, R. C., Allwine, Eugene., Blaha,
689 Denise., Howard, Touche., Guenther, Alex., Lott, R. A., Siverson, Robert., Westburg, Hal., and Zimmerman, Pat.:
690 Development of Atmospheric Tracer Methods To Measure Methane Emissions from Natural Gas Facilities and
691 Urban Areas, *Environ. Sci. Technol.*, 29, 1468–1479, <https://doi.org/10.1021/es00006a007>, 1995.

692 Lavoie, M., Baillie, J., Bourlon, E., O’Connell, E., MacKay, K., Boelens, I., and Risk, D.: Sweet and sour: A
693 quantitative analysis of methane emissions in contrasting Alberta, Canada, heavy oil developments, *Sci. Total
694 Environ.*, 807, 150836, <https://doi.org/10.1016/j.scitotenv.2021.150836>, 2022.

695 MacKay, K., Lavoie, M., Bourlon, E., Atherton, E., O’Connell, E., Baillie, J., Fougère, C., and Risk, D.: Methane
696 emissions from upstream oil and gas production in Canada are underestimated, *Sci. Rep.*, 11, 8041,
697 <https://doi.org/10.1038/s41598-021-87610-3>, 2021.

698 Marriott, R. A., Pirzadeh, P., Marrugo-Hernandez, J. J., and Raval, S.: Hydrogen sulfide formation in oil and gas,
699 *Can. J. Chem.*, 94, 406–413, <https://doi.org/10.1139/cjc-2015-0425>, 2016.

700 Morales, R., Ravelid, J., Vinkovic, K., Korbeń, P., Tuzson, B., Emmenegger, L., Chen, H., Schmidt, M., Humbel, S.,
701 and Brunner, D.: Controlled-release experiment to investigate uncertainties in UAV-based emission
702 quantification for methane point sources, *Atmospheric Meas. Tech.*, 15, 2177–2198,
703 <https://doi.org/10.5194/amt-15-2177-2022>, 2022.

704 Nathan, B. J., Golston, L. M., O’Brien, A. S., Ross, K., Harrison, W. A., Tao, L., Lary, D. J., Johnson, D. R., Covington,
705 A. N., Clark, N. N., and Zondlo, M. A.: Near-Field Characterization of Methane Emission Variability from a
706 Compressor Station Using a Model Aircraft, *Environ. Sci. Technol.*, 49, 7896–7903,
707 <https://doi.org/10.1021/acs.est.5b00705>, 2015.

708 Ocko, I. B., Sun, T., Shindell, D., Oppenheimer, M., Hristov, A. N., Pacala, S. W., Mauzerall, D. L., Xu, Y., and
709 Hamburg, S. P.: Acting rapidly to deploy readily available methane mitigation measures by sector can
710 immediately slow global warming, *Environ. Res. Lett.*, 16, 054042, <https://doi.org/10.1088/1748-9326/abf9c8>,
711 2021.

712 Omara, M., Sullivan, M. R., Li, X., Subramanian, R., Robinson, A. L., and Presto, A. A.: Methane Emissions from
713 Conventional and Unconventional Natural Gas Production Sites in the Marcellus Shale Basin, *Environ. Sci.
714 Technol.*, 50, 2099–2107, <https://doi.org/10.1021/acs.est.5b05503>, 2016.

715 O’Shea, S. J., Allen, G., Gallagher, M. W., Bower, K., Illingworth, S. M., Muller, J. B. A., Jones, B. T., Percival, C. J.,
716 Bauguitte, S. J.-B., Cain, M., Warwick, N., Quiquet, A., Skiba, U., Drewer, J., Dinsmore, K., Nisbet, E. G., Lowry, D.,
717 Fisher, R. E., France, J. L., Aurela, M., Lohila, A., Hayman, G., George, C., Clark, D. B., Manning, A. J., Friend, A. D.,
718 and Pyle, J.: Methane and carbon dioxide fluxes and their regional scalability for the European Arctic wetlands

719 during the MAMM project in summer 2012, *Atmospheric Chem. Phys.*, 14, 13159–13174,
720 <https://doi.org/10.5194/acp-14-13159-2014>, 2014.

721 Pitt, J. R., Allen, G., Bauguitte, S. J.-B., Gallagher, M. W., Lee, J. D., Drysdale, W., Nelson, B., Manning, A. J., and
722 Palmer, P. I.: Assessing London CO₂, CH₄ and CO emissions using aircraft measurements and dispersion modelling,
723 *Atmospheric Chem. Phys.*, 19, 8931–8945, <https://doi.org/10.5194/acp-19-8931-2019>, 2019.

724 Rella, C. W., Tsai, T. R., Botkin, C. G., Crosson, E. R., and Steele, D.: Measuring Emissions from Oil and Natural Gas
725 Well Pads Using the Mobile Flux Plane Technique, *Environ. Sci. Technol.*, 49, 4742–4748,
726 <https://doi.org/10.1021/acs.est.5b00099>, 2015.

727 Riddick, S. N., Connors, S., Robinson, A. D., Manning, A. J., Jones, P. S. D., Lowry, D., Nisbet, E., Skelton, R. L., Allen,
728 G., Pitt, J., and Harris, N. R. P.: Estimating the size of a methane emission point source at different scales: from
729 local to landscape, *Atmospheric Chem. Phys.*, 17, 7839–7851, <https://doi.org/10.5194/acp-17-7839-2017>, 2017.

730 Riddick, S. N., Mauzerall, D. L., Celia, M. A., Kang, M., Bressler, K., Chu, C., and Gum, C. D.: Measuring methane
731 emissions from abandoned and active oil and gas wells in West Virginia, *Sci. Total Environ.*, 651, 1849–1856,
732 <https://doi.org/10.1016/j.scitotenv.2018.10.082>, 2019.

733 Robertson, A. M., Edie, R., Snare, D., Soltis, J., Field, R. A., Burkhart, M. D., Bell, C. S., Zimmerle, D., and Murphy,
734 S. M.: Variation in Methane Emission Rates from Well Pads in Four Oil and Gas Basins with Contrasting Production
735 Volumes and Compositions, *Environ. Sci. Technol.*, 51, 8832–8840, <https://doi.org/10.1021/acs.est.7b00571>,
736 2017.

737 Robertson, A. M., Edie, R., Field, R. A., Lyon, D., McVay, R., Omara, M., Zavala-Araiza, D., and Murphy, S. M.: New
738 Mexico Permian Basin Measured Well Pad Methane Emissions Are a Factor of 5–9 Times Higher Than U.S. EPA
739 Estimates, *Environ. Sci. Technol.*, 54, 13926–13934, <https://doi.org/10.1021/acs.est.0c02927>, 2020.

740 Röckmann, T.: ROMEO-ROmanian Methane Emissions from Oil and Gas, in: EGU General Assembly Conference
741 Abstracts, 18801, 2020.

742 Roscioli, J. R., Yacovitch, T. I., Floerchinger, C., Mitchell, A. L., Tkacik, D. S., Subramanian, R., Martinez, D. M.,
743 Vaughn, T. L., Williams, L., Zimmerle, D., Robinson, A. L., Herndon, S. C., and Marchese, A. J.: Measurements of
744 methane emissions from natural gas gathering facilities and processing plants: measurement methods,
745 *Atmospheric Meas. Tech.*, 8, 2017–2035, <https://doi.org/10.5194/amt-8-2017-2015>, 2015.

746 Rutherford, J. S., Sherwin, E. D., Ravikumar, A. P., Heath, G. A., Englander, J., Cooley, D., Lyon, D., Omara, M.,
747 Langfitt, Q., and Brandt, A. R.: Closing the methane gap in US oil and natural gas production emissions inventories,
748 *Nat. Commun.*, 12, 4715, <https://doi.org/10.1038/s41467-021-25017-4>, 2021.

749 Saunio, M., Stavert, A. R., Poulter, B., Bousquet, P., Canadell, J. G., Jackson, R. B., Raymond, P. A., Dlugokencky,
750 E. J., Houweling, S., Patra, P. K., Ciais, P., Arora, V. K., Bastviken, D., Bergamaschi, P., Blake, D. R., Brailsford, G.,
751 Bruhwiler, L., Carlson, K. M., Carrol, M., Castaldi, S., Chandra, N., Crevoisier, C., Crill, P. M., Covey, K., Curry, C. L.,
752 Etiope, G., Frankenberg, C., Gedney, N., Hegglin, M. I., Höglund-Isaksson, L., Hugelius, G., Ishizawa, M., Ito, A.,
753 Janssens-Maenhout, G., Jensen, K. M., Joos, F., Kleinen, T., Krummel, P. B., Langenfelds, R. L., Laruelle, G. G., Liu,
754 L., Machida, T., Maksyutov, S., McDonald, K. C., McNorton, J., Miller, P. A., Melton, J. R., Morino, I., Müller, J.,
755 Murguía-Flores, F., Naik, V., Niwa, Y., Noce, S., O’Doherty, S., Parker, R. J., Peng, C., Peng, S., Peters, G. P., Prigent,
756 C., Prinn, R., Ramonet, M., Regnier, P., Riley, W. J., Rosentreter, J. A., Segers, A., Simpson, I. J., Shi, H., Smith, S.
757 J., Steele, L. P., Thornton, B. F., Tian, H., Tohjima, Y., Tubiello, F. N., Tsuruta, A., Viovy, N., Voulgarakis, A., Weber,
758 T. S., van Weele, M., van der Werf, G. R., Weiss, R. F., Worthy, D., Wunch, D., Yin, Y., Yoshida, Y., Zhang, W.,
759 Zhang, Z., Zhao, Y., Zheng, B., Zhu, Q., Zhu, Q., and Zhuang, Q.: The Global Methane Budget 2000–2017, *Earth
760 Syst. Sci. Data*, 12, 1561–1623, <https://doi.org/10.5194/essd-12-1561-2020>, 2020.

761 Shah, A., Ricketts, H., Pitt, J. R., Shaw, J. T., Kabbabe, K., Leen, J. B., and Allen, G.: Unmanned aerial vehicle
762 observations of cold venting from exploratory hydraulic fracturing in the United Kingdom, *Environ. Res.
763 Commun.*, 2, 021003, <https://doi.org/10.1088/2515-7620/ab716d>, 2020.

764 Shen, L., Zavala-Araiza, D., Gautam, R., Omara, M., Scarpelli, T., Sheng, J., Sulprizio, M. P., Zhuang, J., Zhang, Y.,
765 Qu, Z., Lu, X., Hamburg, S. P., and Jacob, D. J.: Unravelling a large methane emission discrepancy in Mexico using
766 satellite observations, *Remote Sens. Environ.*, 260, 112461, <https://doi.org/10.1016/j.rse.2021.112461>, 2021.

767 Shi, T., Han, Z., Han, G., Ma, X., Chen, H., Andersen, T., Mao, H., Chen, C., Zhang, H., and Gong, W.: Retrieving
768 CH₄-emission rates from coal mine ventilation shafts using UAV-based AirCore observations and the genetic
769 algorithm–interior point penalty function (GA-IPPF) model, *Atmospheric Chem. Phys.*, 22, 13881–13896,
770 <https://doi.org/10.5194/acp-22-13881-2022>, 2022.

771 Szopa, S., Naik, V., Adhikary, B., Artaxo, P., Berntsen, T., Collins, W. D., Fuzzi, S., Gallardo, L., Kiendler-Scharr, A.,
772 Klimont, Z., Liao, H., Unger, N., and Zanis, P.: Short-Lived Climate Forcers, *Clim. Change 2021 Phys. Sci. Basis*
773 *Contrib. Work. Group Sixth Assess. Rep. Intergov. Panel Clim. Change Camb. Univ. Press Camb. U. K. N. Y. NY USA*,
774 817–922, 2021.

775 Thoma, E. and Squier, B.: OTM 33 geospatial measurement of air pollution, remote emissions quantification
776 (gmap-req) and OTM33A geospatial measurement of air pollution-remote emissions quantification-direct
777 assessment (GMAP-REQ-DA), *US Environ. Prot. Agency Cincinnati OH*, 2014.

778 Tuzson, B., Graf, M., Ravelid, J., Scheidegger, P., Kupferschmid, A., Looser, H., Morales, R. P., and Emmenegger,
779 L.: A compact QCL spectrometer for mobile, high-precision methane sensing aboard drones, *Atmospheric Meas.*
780 *Tech.*, 13, 4715–4726, <https://doi.org/10.5194/amt-13-4715-2020>, 2020.

781 Tyner, D. R. and Johnson, M. R.: Where the Methane Is—Insights from Novel Airborne LiDAR Measurements
782 Combined with Ground Survey Data, *Environ. Sci. Technol.*, 55, 9773–9783,
783 <https://doi.org/10.1021/acs.est.1c01572>, 2021.

784 Greenhouse Gas Inventory Data - Comparison by Category: https://di.unfccc.int/comparison_by_category, last
785 access: 2 November 2022.

786 Vinković, K., Andersen, T., de Vries, M., Kers, B., van Heuven, S., Peters, W., Hensen, A., van den Bulk, P., and
787 Chen, H.: Evaluating the use of an Unmanned Aerial Vehicle (UAV)-based active AirCore system to quantify
788 methane emissions from dairy cows, *Sci. Total Environ.*, 831, 154898,
789 <https://doi.org/10.1016/j.scitotenv.2022.154898>, 2022.

790 Yacovitch, T. I., Daube, C., Vaughn, T. L., Bell, C. S., Roscioli, J. R., Knighton, W. B., Nelson, D. D., Zimmerle, D.,
791 Pétron, G., and Herndon, S. C.: Natural gas facility methane emissions: measurements by tracer flux ratio in two
792 US natural gas producing basins, *Elem. Sci. Anthr.*, 5, 69, <https://doi.org/10.1525/elementa.251>, 2017.

793 Yacovitch, T. I., Neiningner, B., Herndon, S. C., van der Gon, H. D., Jonkers, S., Hulskotte, J., Roscioli, J. R., and
794 Zavala-Araiza, D.: Methane emissions in the Netherlands: The Groningen field, *Elem. Sci. Anthr.*, 6, 57,
795 <https://doi.org/10.1525/elementa.308>, 2018.

796 Zavala-Araiza, D., Lyon, D. R., Alvarez, R. A., Davis, K. J., Harriss, R., Herndon, S. C., Karion, A., Kort, E. A., Lamb, B.
797 K., Lan, X., Marchese, A. J., Pacala, S. W., Robinson, A. L., Shepson, P. B., Sweeney, C., Talbot, R., Townsend-Small,
798 A., Yacovitch, T. I., Zimmerle, D. J., and Hamburg, S. P.: Reconciling divergent estimates of oil and gas methane
799 emissions, *Proc. Natl. Acad. Sci.*, 112, 15597–15602, <https://doi.org/10.1073/pnas.1522126112>, 2015.

800 Zavala-Araiza, D., Alvarez, R. A., Lyon, D. R., Allen, D. T., Marchese, A. J., Zimmerle, D. J., and Hamburg, S. P.:
801 Super-emitters in natural gas infrastructure are caused by abnormal process conditions, *Nat. Commun.*, 8, 14012,
802 <https://doi.org/10.1038/ncomms14012>, 2017.

803 Zavala-Araiza, D., Herndon, S. C., Roscioli, J. R., Yacovitch, T. I., Johnson, M. R., Tyner, D. R., Omara, M., and
804 Knighton, B.: Methane emissions from oil and gas production sites in Alberta, Canada, *Elem. Sci. Anthr.*, 6, 27,
805 <https://doi.org/10.1525/elementa.284>, 2018.

806 Zavala-Araiza, D., Omara, M., Gautam, R., Smith, M. L., Pandey, S., Aben, I., Almanza-Veloz, V., Conley, S.,
807 Houweling, S., Kort, E. A., Maasakkers, J. D., Molina, L. T., Pusuluri, A., Scarpelli, T., Schwietzke, S., Shen, L., Zavala,

808 M., and Hamburg, S. P.: A tale of two regions: methane emissions from oil and gas production in
809 offshore/onshore Mexico, *Environ. Res. Lett.*, 16, 024019, <https://doi.org/10.1088/1748-9326/abceeb>, 2021.